

Effect of Acetic Acid on the Pitting Corrosion of 2Cr12MoV Turbine Steel in Early Condensates Containing Chloride Ions

*Jiaqiang Wei, Baiqing Zhou**

School of Power and Mechanical Engineering, Wuhan University, No.8 South East Lake Road, Wuchang District, Wuhan City, Hubei Province, 430072, People's Republic of China

*E-mail: zhoubaiqing5@163.com

Received: 26 January 2017 / Accepted: 19 February 2017 / Published: 12 March 2017

The effect of acetic acid on the pitting corrosion of 2Cr12MoV turbine steel in early condensates containing chloride ions was investigated by potentiodynamic and potentiostatic polarization, scanning electron microscopy, energy dispersive X-ray spectroscopy and electrochemical impedance spectroscopy. The potentiodynamic polarization tests results illustrate acetic acid decreased the metastable pitting and pitting potentials. The potentiostatic polarization tests and scanning electron microscopy, energy dispersive X-ray spectroscopy results revealed acetic acid promoted the pits initiation and propagation. The electrochemical impedance spectroscopy indicated acetic acid increased corrosion rate and decreased the pitting corrosion resistance.

Keywords: Blade steel, pitting corrosion, Acetic acid, Early condensate

1. INTRODUCTION

In low pressure (LP) steam turbines of power plants, steam cools and partitions into liquid and vapor phases during adiabatic expansion, liquid phase then formed condensed water droplets in the phase transition zone (PTZ) [1-3]. Impurities such as Cl⁻ and organic acid transporting from vapor phases to the liquid phase concentrated in condensed water droplets due to their low distribution coefficients [1-5]. The concentrated solutions are termed "early condensates". Most outage hours for steam turbines are due to corrosion of low pressure (LP) blades and disks in the phase transition zone (PTZ) of LP steam turbines. Many studies and field observations have shown that the early condensates can cause significant corrosion damage in turbine environments, including stress corrosion cracking (SCC) and pitting of blades, discs, and rotors [6-8].

Chloride ions as aggressive anion concentrated in early condensate causing pitting corrosion for turbine steel have studied in some previous research [9-11]. Acetic acid (HAc) is the principal organic acid in the early condensate, according to the investigation of impurities in PTZ [1-2], the concentration of acetic acid in the early condensate is more than 1000 times higher than that in inlet steam and that can result in a depressed pH in early condensate. The effect of HAc on the corrosion of metal has been studied by many researchers. Some researchers reported HAc accelerated metal corrosion and pitting corrosion in CO₂ corrosion of metal [12-17], W.Y. Maeng et al, also reported the stress corrosion cracking susceptibility increasing with increasing HAc concentration [18]. However, the effect of acetic acid in conjunction with the chloride on pitting corrosion in early condensates are few studied and not well understood. In the present work, the effect of acetic acid on the pitting corrosion of 2Cr12MoV turbine steel in early condensates containing chloride ions was studied by electrochemical measurements and pit morphology analyses. This work first insight into the mechanism of the effect of HAc on the pitting corrosion in early condensates containing chloride ions and improving the understanding of this impact can help plants better assess the risks of turbine corrosion.

2. EXPERIMENT

2.1 Materials And Solution

2Cr12MoV blade steel was used for this study with a chemical composition: 0.20% C, 0.21% Si, 0.76% Mn, 0.012% P, 0.011% S, 0.007% Cr, 11.89% Mo, 0.83% Ni, 0.06% Cu, and Fe balance. The electrodes for electrochemical tests were embedded in epoxy resin with exposed working area of 1.0 cm². Prior to testing, working electrodes were polished on successively grades of metallographic sandpaper up to 1200 grit, then washed by deionized water and degreased with acetone.

In this work, test solutions based on the quality of early condensate [1-3] with a constant chloride ions and various HAc concentration, which shown in Table 1. The test temperature was 90°C. Besides, before the tests, the solution was deoxygenated by purging pure N₂ until the concentration of dissolved oxygen below 5ppb.

Table 1. Quality of test solution

Test solution No.	Impurities concentration (ppm)		Conductivity (90°C)	pH (90°C)
	Cl ⁻	HAc		
1	10	0	81.2	7.00
2	10	10	110.7	4.39
3	10	50	152.5	4.00
4	10	100	183.8	3.84

2.2 Electrochemical Measurements

Electrochemical measurements, including potentiodynamic polarization, potentiostatic polarization and electrochemical impedance spectroscopy (EIS), were carried out using a CS350 electrochemical workstation with a three-electrode system: The 2Cr12MoV blade steel was used as working electrode, while both Pt electrodes were used as the counter electrode and reference electrode. It should be pointed out that in this work, Pt electrode instead of the conventional reference electrode, i.e. saturated calomel electrode or Ag/AgCl electrode, adopted as the reference electrode. The reason is that impurities concentration and conductivity of test solution in this work is low, if saturated calomel electrode or Ag/AgCl electrode adopted as the reference electrode, chloride ions would contamination test solution by due to the diffusion of chloride ions from the reference electrode chamber to the test cell occurred during the test. Prior to electrochemical measurements, the test solution was deoxygenated by purging pure N₂ for 1 h. Electrode was then immersed into solution and N₂ purging was continued throughout the tests at a low flow rate at the headspace but (to avoid flow effects) not bubbled through the electrolyte.

Potentiodynamic polarization tests were begun at a potential 200 mV below the open circuit potential and with a scan rate of 0.2 mV/s in anodic direction until the current density reached 400 $\mu\text{A}/\text{cm}^2$. The potential corresponding to the first current peak in passive region of Potentiodynamic polarization curve called metastable pitting potential E_m [19-20], and the potential at which the current density reached 10 $\mu\text{A}/\text{cm}^2$ used as an approximation of the pitting potential E_p [11,21]. The values of E_m and E_p potentials for 2Cr12MoV blade steel in different test solution recorded.

Potentiostatic polarization tests were then conducted for 24 h in the four test solution. The applied potentials were the E_p potential obtained in the absence of HAc test solution with only 10 ppm Cl⁻ and in that 10 ppm Cl⁻ and 100 ppm HAc. After the potentiostatic polarization tests, the specimens were observed with, an optical microscope (OM), a scanning electron microscope (SEM). SEM observations and elemental analyses with energy-dispersive X-ray spectroscopy (EDS) were also conducted on the pits found on specimens. For the EDS analyses, point analysis was performed on the corrosion products inside the pit.

The electrochemical impedance spectroscopy (EIS) measurements were carried out at OCP under perturbation amplitude of 10 mV and the measuring frequency from 100 kHz to 0.01 Hz.

3. RESULTS AND DISCUSSION

3.1 Potentiodynamic polarization

Figure 1 shows the potentiodynamic polarization curves for 2Cr12MoV steel in the test solutions at 90 °C. In the Figure 1, E_{m1} , E_{m2} , E_{m3} , E_{m4} correspond to the metastable pitting potential of 2Cr12MoV steel in 10 ppm Cl⁻ solution with 0 ppm, 10 ppm, 50ppm, 100ppm HAc, respectively. E_{p1} , E_{p2} , E_{p3} , E_{p4} correspond to pitting potential, respectively. The values of metastable pitting and pitting potentials obtained from the potentiodynamic polarization curves shown in Figure 2. Both E_m

and E_p shifted to negative values in the test solution with added HAC and decreased with HAC concentration increasing.

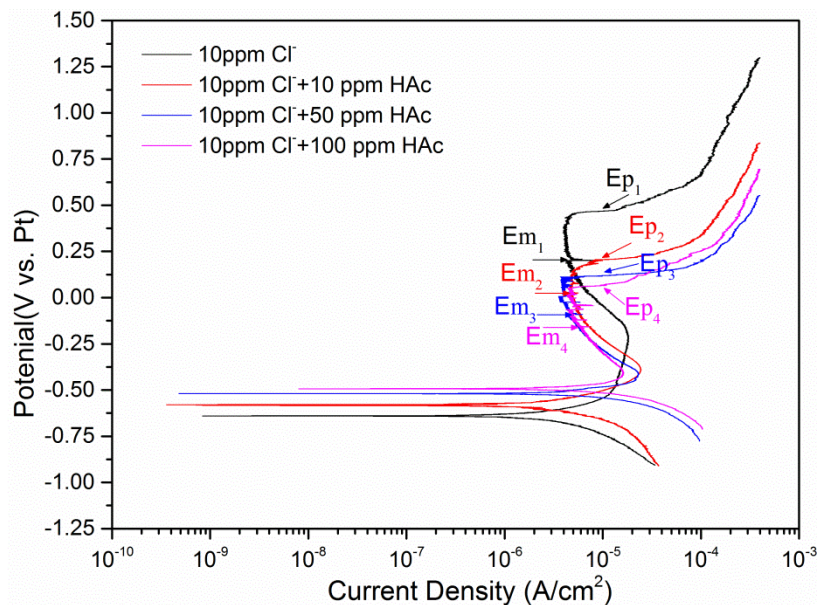


Figure 1. Potentiodynamic polarization curves of 2Cr12MoV steel in the different test solutions.

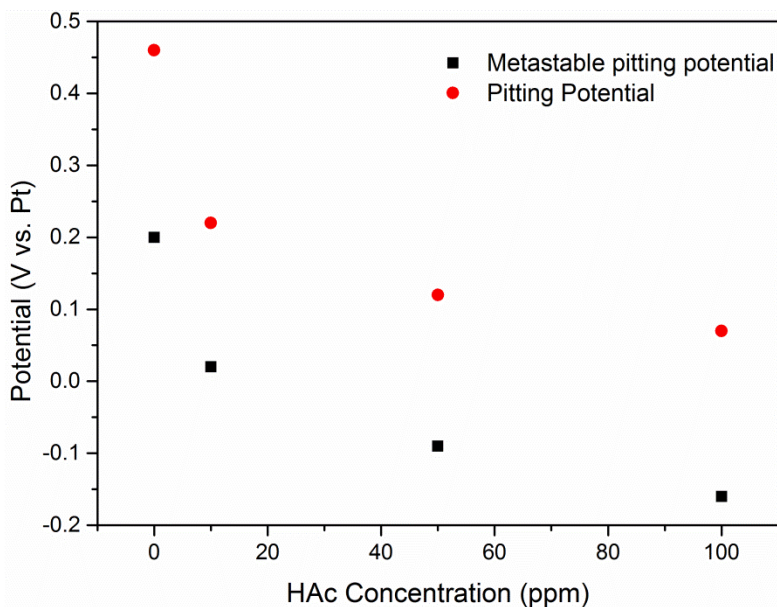


Figure 2. The values of metastable pitting and pitting potentials for 2Cr12MoV steel vary with HAC concentration in test solution.

Cl^- ions are well known to be aggressively ions cause pitting corrosion on steels. It has been reported that the presence of HAC in solution containing Cl^- accelerate pitting corrosion [14-17]. In this work, solution pH decreased and conductivity increased with HAC concentration increasing. Thus, the corrosion resistance and the stability of passive film decreased with increasing HAC concentration.

Therefore, the E_m and E_p shifted to negative values with HAc concentration increasing. The localised acidification model [22-25] support these results: because the critical value x_i depend on pH and the metal dissolution rate inside the pit increased with HAc concentration increasing, therefore a lower potential needed to activate a pit with HAc concentration increasing.

3.2 Potentiostatic polarization

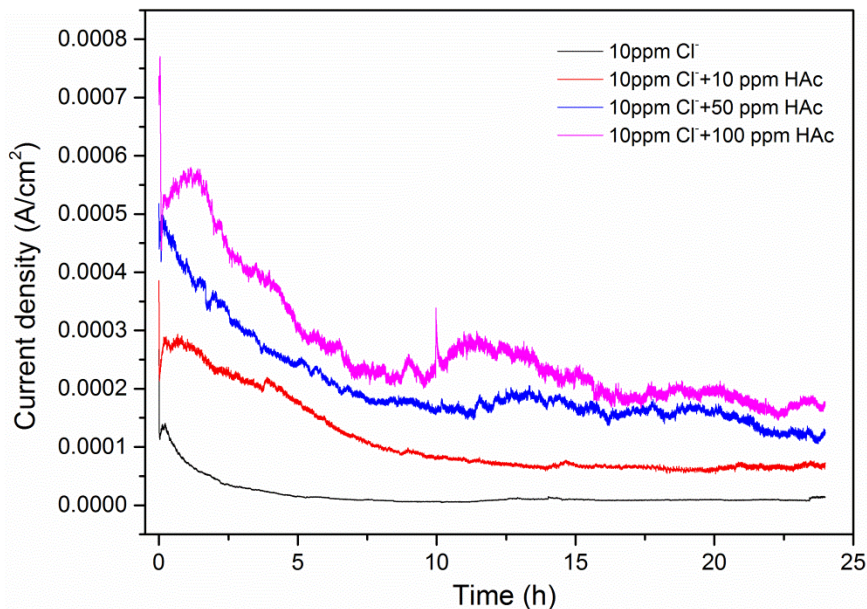


Figure 3. Current density varies with time for 2Cr12MoV steel in different test solution during potentiostatic polarization at applied 0.47 V (vs. Pt).

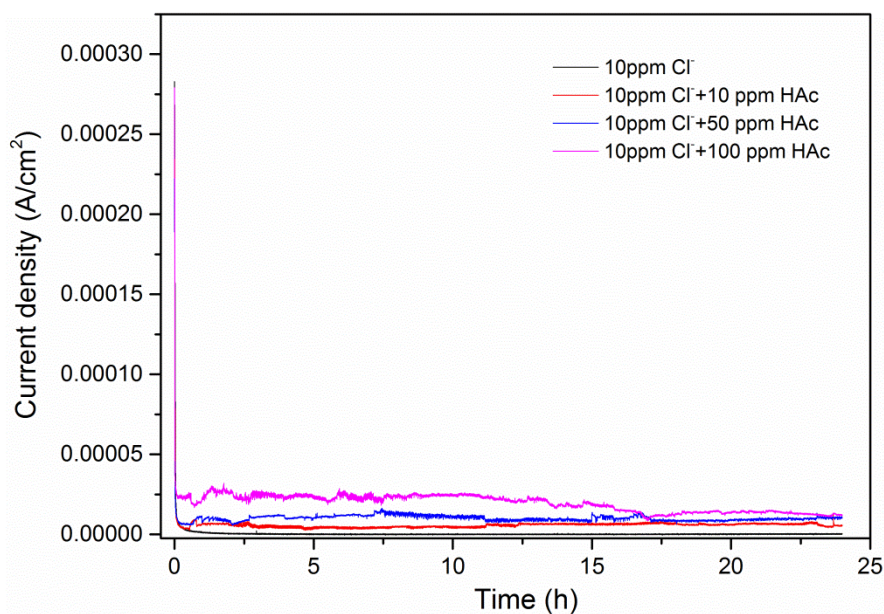


Figure 4. Current density varies with time for 2Cr12MoV steel in different test solution during potentiostatic polarization at applied 0.07 V (vs. Pt).

Potentiostatic polarization tests were conducted in test solution at the applied potentials of 0.47 V (vs. Pt) and 0.07 V (vs. Pt). The applied potentials were the E_p of 2Cr12MoV steel in the test solution with 10 ppm Cl^- and both 10 ppm Cl^- and 100 ppm HAc, respectively. Figure 3 and 4 shows the current density varies with time for 2Cr12MoV steel in different test solution during potentiostatic polarization at applied 0.47 V (vs. Pt) and 0.07 V (vs. Pt), respectively. At both applied potentials, the current density of 2Cr12MoV steel increased with HAc concentration increasing, this indicates pits nucleation rates and growth rates increased with HAc concentration increasing.

At the applied potential of 0.47 V (vs. Pt), as the potential higher than E_p in all test solution the current density varies with time during potentiostatic polarization at applied 0.47 V (vs. Pt) influenced by the growth of passive layer, pit initiated and propagated: At first, current density quickly decreases at t_i due to the growth of the passive layer on the electrode surface, the pitting time related to the rate of pit nucleation [26-29]; After t_i , the pits initiated and grow to become stable pits, current density increases; Then pits propagated, as the propagation of pits is diffusion controlled, the current density gradually decreases with time due to pits growth suppressed by corrosion products gradually formed inside the pits and covering the pit mouths [11, 22, 30]. Because of salts products can't suppress the pits propagated absolutely, pits will still propagated at a low growth rate after some time and current density decreases to steady state values. In addition, once pits initiated after t_i , current density would have an oscillation due to pits initiated and then repassivated.

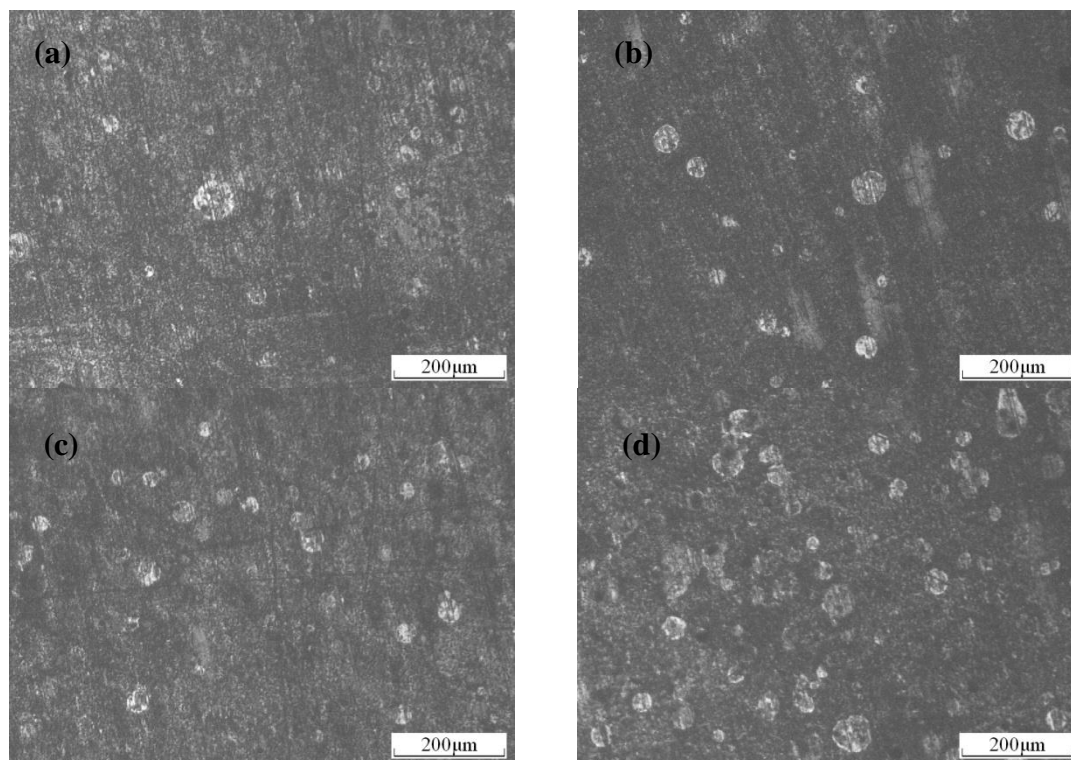


Figure 5. Appearance of specimens after potentiostatic polarization at 0.47 V (vs. Pt) in test solution with (a) 10 ppm Cl^- , (b) 10 ppm Cl^- + 10 ppm HAc, (c) 10 ppm Cl^- + 50 ppm HAc, (d) 10 ppm Cl^- + 100 ppm HAc.

As shown in Figure 3, current density increased with HAc concentration increasing at all time, this indicated HAc accelerate 2Cr12MoV steel pitting corrosion in the early condensates containing chloride ions. Current density increased with HAc concentration increasing at all time due to HAc decreasing the growth rate of passive layer and weaker the passive layer before pits initiated, increasing pits nucleation rates and growth rates when pits initiated and propagated. The effect of HAc concentration on the pitting process interpreted as below: At first, with an increase in HAc concentration, the passive layer tends to dissolve to metal ions; After t_i , as E_m and E_p decreased with HAc concentration increasing, more pits initiated and activated to stable pits; When pits propagated after some time and under diffusion control, because of the conductivity of test solution increased with HAc concentration increasing, the metal ions transfer out pits quickly with HAc concentration increasing, pitting corrosion rate increased with HAc concentration increasing. Therefore, Current density increased with HAc concentration increasing.

Figure 5 shows the appearance of 2Cr12MoV steel after potentiostatic tests at 0.47 V (vs. Pt) in test solution. At the applied potential of 0.47 V (vs. Pt), as the potential higher than E_p in all test solution, the pit would initiated and propagated. The pitting corrosion was evident in all test solution as shown in Figure 5. As shown in Figure 6, the pitting number density increased with HAc concentration increasing. Therefore, it is considered that more metastable pits initiated and grow to become stable pits with an increase of HAc concentration. These consist with above results.

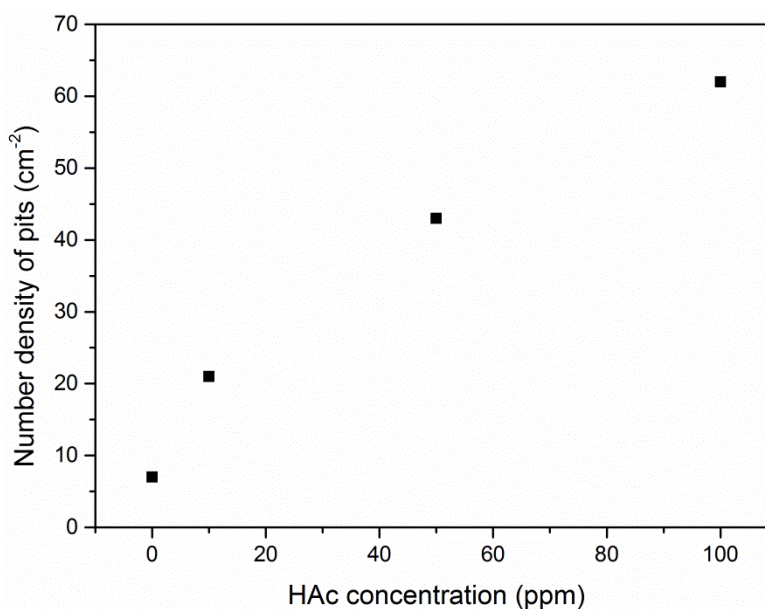


Figure 6. Number density of pits on specimens after potentiostatic polarization at 0.47V (vs. Pt) varies with HAc concentration.

At the applied potential of 0.07 V (vs. Pt), as the potential lower than the E_m and E_p in the test solution containing 10 ppm Cl^- in the absence of HAc, current density decreases to zero due to passive layer and without pit initiated. However, the applied potential higher than E_m in the other test solution in the presence of HAc. Current density varies with time in test solution in the presence of HAc similar

with that at 0.47 V (vs. Pt) and the Current density increased with HAC concentration increasing. This result consists with potentiodynamic polarization and potentiostatic polarization at 0.47 V (vs. Pt) results and HAC accelerate 2Cr12MoV steel pitting corrosion.

3.3 Morphology and pit growth behavior

The effect of HAC on the pit morphology and pit growth behavior of 2Cr12MoV steel in early condensates containing 10 ppm Cl^- was investigated using the specimens from the potentiostatic polarization at the applied potential of 0.47 V (vs. Pt). Figure 7 shows the SEM micrographs of typical pits on the specimens after the potentiostatic polarization at the applied potential of 0.47 V (vs. Pt). With an increase in HAC concentration in the test solution, the number of pits on the specimens increased and the shape and size of pits changed. The pits formed in the free of HAC test solution and 10 ppm, 50 ppm HAC added test solution gradually larger but independent, as shown in Figure 7 (a), (b) and (c), but the pits formed in the test solution added 100 ppm HAC not only larger but also connect with some other small pits, as shown in Figure 7(d).

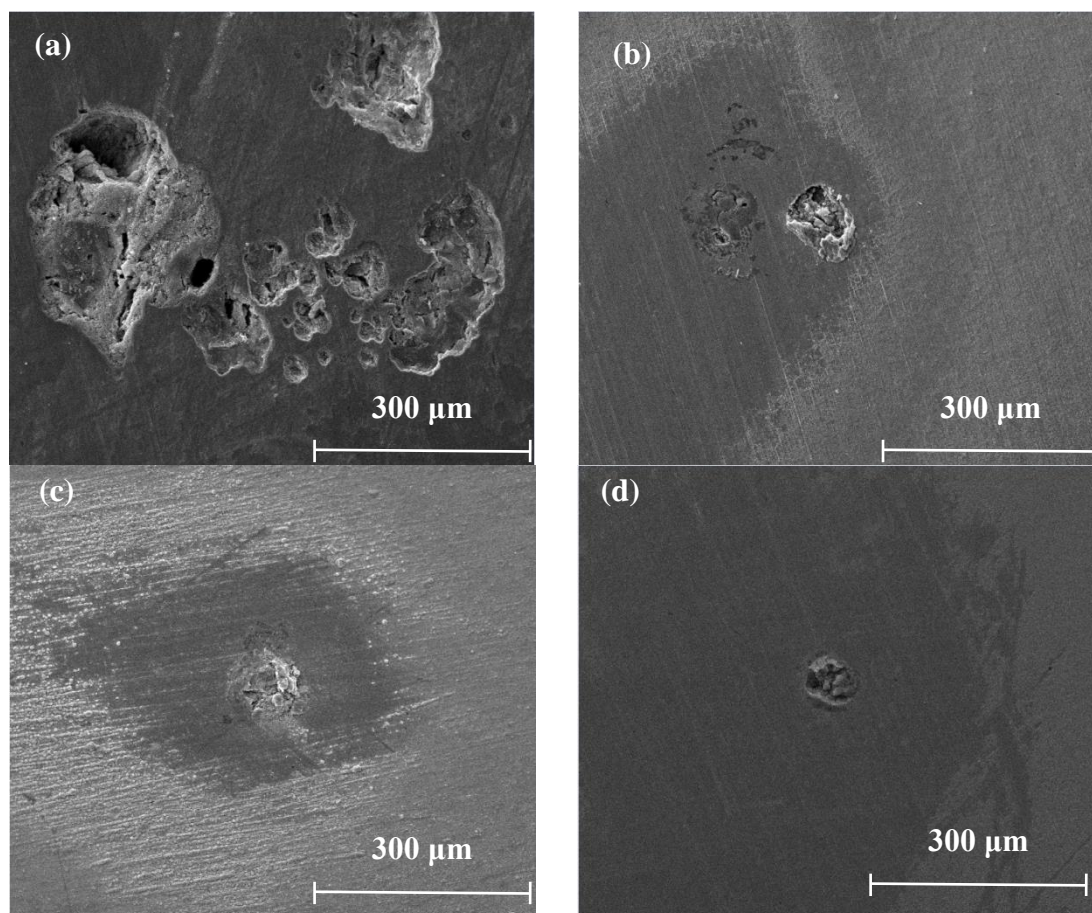
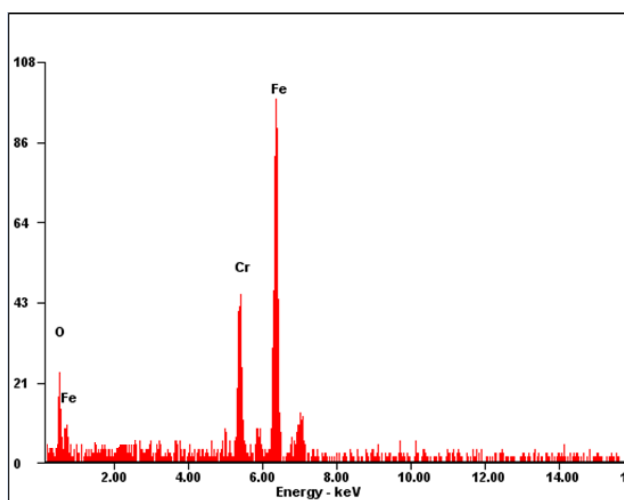


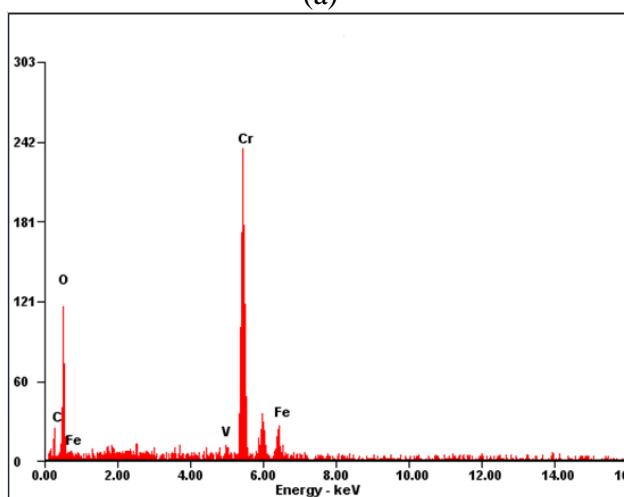
Figure 7. Typical pits on the specimens after potentiostatic polarization at 0.47 V (vs. Pt) in test solution with (a) 10 ppm Cl^- , (b) 10 ppm Cl^- + 10 ppm HAC, (c) 10 ppm Cl^- + 50 ppm HAC, (d) 10 ppm Cl^- + 100 ppm HAC.

We also can see from Figure 7 the corrosion products were observed inside the pits and covered a part of pits mouth in all test solution. It is demonstrated pits growth suppressed by corrosion products inside the pits and covering the pit mouths which consist with the potentiostatic tests.

Figure 8 shows the EDS spectra of the corrosion products inside the pits on the specimens after the potentiostatic polarization at the applied potential of 0.47 V (vs. Pt). As shown in Figure 8(a), the main elements inside the pits (Figure 7(a)) formed in the test solution in the absence of HAC are Fe, Cr, and O. It is indicate that Cr-oxides and Fe-oxides formed inside such pits. However, the elements inside the pits (Figure 7(b)) formed in the test solution in the presence of 10 ppm HAC and the pits (Figure 7(d)) formed in the test solution in the presence of 100 ppm HAC are a large amount of Fe, Cr, O, and C, and a large amount of Fe, Cr, O, C and a small amount of Cl, respectively. C may come form HAC due to HAC participation in corrosion process and Cl concentrated inside pits in the test solution in the presence 100 ppm HAC due to high metal dissolution rate, more chloride ions migrate form bulk solution into the pits to keep electric neutrality.



(a)



(b)

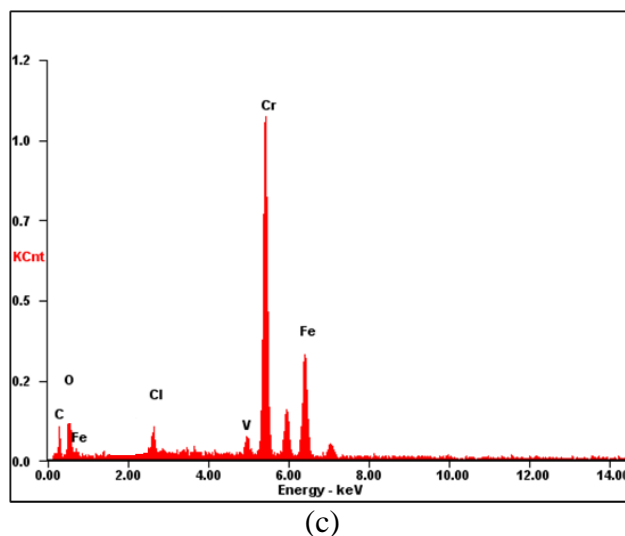


Figure 8. EDS spectra for corrosion products of inside pits on the specimens after potentiostatic polarization at 0.47 V (vs. Pt) in test solution with (a) 10 ppm Cl^- , (b) 10 ppm Cl^- + 10 ppm HAC, (c) 10 ppm Cl^- + 100 ppm HAC.

Since pits formed in the test solution influenced by HAC concentration, it is concluded that HAC play a key role in the initiation and propagation of a pit. The related pitting mechanisms are described as below: Before pits formed or during the pits incubation, the passive layer formed on the surface of steel, Since HAC decrease the stability of passive layer and increase metal dissolution inside the pits, the criterion for stable pit growth more easily reached [22]. Thus more metastable pits initiated and grow to stable pits. In the initial stage of propagation, the insides of pit are anodic sites where metal dissolution takes place. To keep electric neutrality, chloride ions must migrate form bulk solution into the pit. HAC also migrate form bulk solution into the pit under the effect of concentration differences due to HAC depletion inside the pit when HAC presence in test solution [16, 22, 30]. Therefore, the chloride ions and HAC may gradually accumulate around the anodic sites, leading to high concentration at the pit mouth. The chloride ions and HAC either form salt products with ferrous ions or diffuse away. When HAC concentration high in the test solution, the sites where chloride ions and HAC reach will immediately become an anodic site, the diffusion of chloride ion and HAC towards all directions from the pit mouth causing the pit shape larger, pits may connect with some small pits, as shown in Figure 7(d). However, when the test solution in the absence of HAC or the concentration of HAC low, the site where a chloride ions reaches will remain passivated due to lack of critical chemistry that essential for pit initiated and propagated, thus the pits independent with other pits. This illustrates the morphology of pits depend on HAC concentration.

3.4 EIS

Figure 9 shows the Nyquist diagrams of 2Cr12MoV turbine steel in test solution. It is seen that there are two capacitive arc in both test solutions, which is related to the resistance of the passive layer. Many different models have used explain impedance spectra on a passive metal surface. On the basis of previous references [17, 31-33], the equivalent circuit shown Figure 10 was used to fit the

experimental impedance data. For the equivalent electric circuit, where R_s represents solution resistance, CPE1 is constant phase element to represents the capacitance of passive layer on the surface of 2Cr12MoV turbine steel, R_p represents the pitting corrosion resistance or the resistance to ionic current through the pits, it related to the point defect on the passive layer, C1 represents the double layer capacitance and R_t represents charge transfer resistance. The fitting results are shown in Table 2.

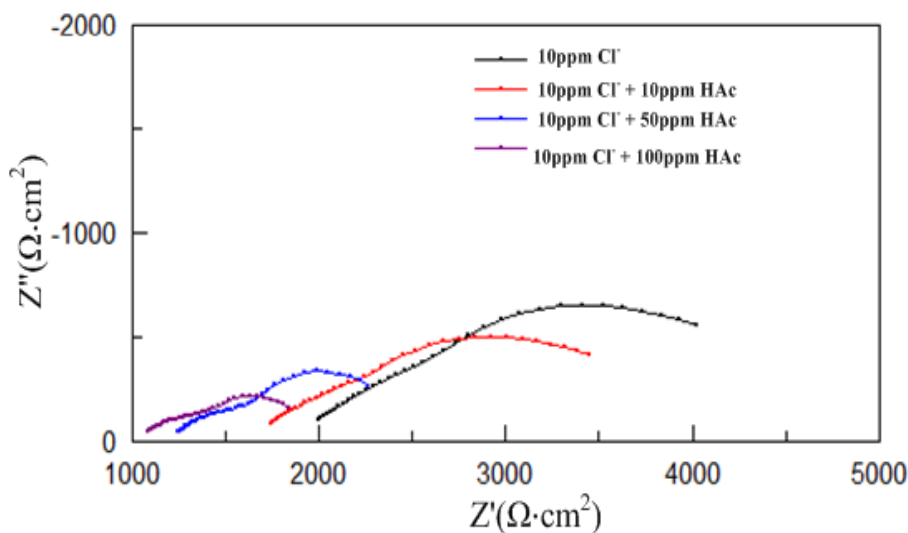


Figure 9. Nyquist diagrams of 2Cr12MoV turbine steel in different test solution.

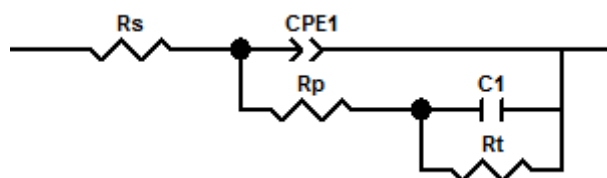


Figure 10. Equivalent electrical circuit of Nyquist diagrams.

Table 2. EIS parameters for 2Cr12MoV blade steel in the test solution with different concentration of HAc.

Parameters	0 ppm	10 ppm	50 ppm	100 ppm
$R_s (\Omega \cdot \text{cm}^2)$	1869	1621	1185	1012
$\text{CPE1-}Y_0 / (\Omega \cdot \text{s}^n \cdot \text{cm}^2)$	0.00054467	0.00057196	0.00080192	0.00091821
CPE1-n	0.45503	0.42339	0.45668	0.42848
$R_p (\Omega \cdot \text{cm}^2)$	2038	1819	803.1	704.9
$C1 (\text{F} \cdot \text{cm}^2)$	0.0014108	0.0013412	0.0055352	0.0081784
$R_t (\Omega \cdot \text{cm}^2)$	1103	811.7	641.1	357.7

According to Table 2, with added HAc and an increase in the concentration of HAc in test solution, R_t gradually decreased which indicates the corrosion of solution gradually increased,

corrosion rate increased with increasing HAc concentration. At the same time, R_p also decreased, it indicates pitting corrosion resistance decreased, i.e., pits nucleation and growth rate increased with increasing HAc concentration. The results consist with the potentiodynamic and potentiostatic polarization.

4. CONCLUSIONS

The effect of acetic acid on the pitting corrosion of 2Cr12MoV turbine steel in early condensates containing chloride ions have been explored in this study. The results show HAc play a key role in the initiation and propagation of a pit in early condensates. HAc increases corrosion rate and decreases pitting corrosion resistance of 2Cr12MoV turbine steel in early condensates containing chloride ions. With an increase in HAc concentration, metastable pitting and pitting potentials shifted to negative values and pits nucleation rates and growth rates increases. The number density of pits on the specimens increased and the size of pits larger with increasing HAc concentration.

References

1. O. Jonas, Steam, *EPRI*, Report TR-108184-V1 (1999).
2. O. A. Povarov, T.I. Petrova and V.N. Semenov, *EPRI*, Report TR-113090 (1999).
3. S. Zhou, A. Turnbull. *Corros. Eng. Sci. Technol.*, 38 (2003) 7-115.
4. O. Jonas. *Int. Joint. Power. Gen. Conf.*, (1998).
5. M. Wispelaere, 14th International Conference on the Properties of Water and Steam, Kyoto, Japan. Vol. 602, (2004).
6. F. J. Heyman, V. P. Swaminathan and J. W. Cunningham, *EPRI*, Palo Alto, CA. Report CS-1967, (1967).
7. S. Zhou, A. Turnbull. *Corros. Eng. Sci. Technol.*, 38 (2003) 177-191.
8. C. Wells, D. Rosario and B. Dooley. *EPRI*, Palo Alto, CA. TR-111340, (1999).
9. *EPRI*, Palo Alto, CA. Report 000000000001023196, (2011).
10. G. Williams, H. N. McMurray. *Corrosion.*, 62 (2006) 231.
11. L. B. Niu, K. Nakada, *Corros. Sci.*, 96 (2015) 171.
12. M. M. Singh, A. Gupta, *Corrosion.*, 56 (2000) 371.
13. A. Kahyarian, B. Brown and S. Nešić, *Corrosion*, 72 (2016) 1539.
14. Z. F. Yin, Y. R. Feng, W. Z. Zhao, C. X. Yin and W. Tian, *Corros. Eng. Sci. Technol.*, 46 (2011) 56.
15. J. Amri, E. Gulbrandsen, R. P. Nogueira, *Electrochem. Commun.*, 10 (2008) 200.
16. J. Amri, E. Gulbrandsen, R. P. Nogueira, *Electrochimica Acta*, 54 (2009) 7338.
17. Z. F. Yin, W. Z. Zhao, W. Tian, Y. R. Feng and C. X. Yin. *J. Solid. State. Electrochem.*, 13 (2009) 1291.
18. W. Y. Maeng, Digby D. Macdonald, *Corros. Sci.*, 50 (2008) 2239.
19. G. S. Frankel, L. Stockert, F. Hunkeler and H. Boehni, *Corrosion.*, 43 (1987) 429.
20. Y. Tang, Y. Zuo, J. Wang, X. Zhao, B. Niu and B. Lin, *Corros. Sci.* 80 (2014) 111.
21. Japan Society of Corrosion Engineering, Corrosion Handbook, Maruzen, (2000) Tokyo, Japan.
22. P. C. Pistorius, G. T. Burstein, *Philosophical Transactions of the Royal Society of London A: Mathematical, Physical and Engineering Sciences*, 341 (1992) 531.
23. J. R. Galvele, *J. Electrochem. Soc.*, 123 (1976) 464.

24. R. Newman, *Electrochem. Soc. Interf.* 2 (2010) 32.
25. J. Soltis, *Corros. Sci.*, 5 (2015) 90.
26. C. Y. Chao, L. F. Lin and D. D. Macdonald, *J. Electrochem. Soc.*, 128 (1981) 1187.
27. D. D. Macdonald, M. J. Urquidi-Macdonald, *J. Electrochem. Soc.*, 137 (1990) 2395.
28. A. Broli, H. Holtan and T. B. Andreassen, *Mater. Corros.*, 27 (1976) 497.
29. H. H. Hassan, K. Fahmy, *Int. J. Electrochem. Sci.*, 3 (2008) 29.
30. Y. F. Wang, G. G. Cheng, W. Wu, Q. Qiao, Y. Li and X. F. Li, *Appl. Surf. Sci.* 349 (2015) 746.
31. L. Li, C. F. Dong, K. Xiao, J. Z. Yao and X. G. Li, *Constr. Build. Mater.* 68 (2014) 709.
32. B. Gyitián, X.R. Nóvoa and B. Puga. *Electrochim Acta.*, 56 (2011) 7772.
33. V. Gyitián -Pina, A. Igual- Gyitián and J. García-Antón, *Corros. Sci.*, 53 (2011) 575.

© 2017 The Authors. Published by ESG (www.electrochemsci.org). This article is an open access article distributed under the terms and conditions of the Creative Commons Attribution license (<http://creativecommons.org/licenses/by/4.0/>).